JACS
JOURNAL OF THE AMERICAN CHEMICAL SOCIETY
pubs.acs.org/JACS
Article

Chiral Porous Sheet Assembly for Multiple Chirality Induction in Macrocycle Formation

Yongsheng Li, Tianyi Zheng, Zhanting Li,* Young Yong Kim, and Myongsoo Lee*

Cite This: J. Am. Chem. Soc. 2025, 147, 31198−31203
Read Online

ABSTRACT: The stereochemistry of chiral macrocycles bearing multiple chirality has a crucial influence on their physical and biological properties. Nevertheless, the multiple chirality induction in macrocyclizations remains largely unexplored in the synthetic community. Here we report that confined macrocyclizations in single-layer chiral porous sheets can generate macrocyclic products bearing multiple chirality with excellent stereoselectivity. To induce multiple chirality in a confined macrocyclization, we used chiral porous sheet structures formed through the self-assembly of a planar aromatic amphiphile including a tilt rod. The chiral interior of the porous sheet imprints its stereochemistry on the conformation of a linear substrate, enabling the ring closing reaction to simultaneously induce multiple chirality, including a stereocenter and strain-induced chirality.

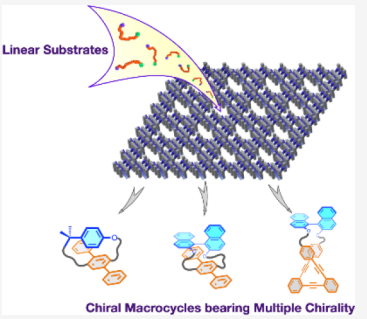

INTRODUCTION

Complex macrocycles bearing multiple chirality are commonly found in nature and possess a wide range of biological activities.[1−4] The stereochemical configuration together with the conformational rigidity associated with closed ring structures has a tremendous impact on their physical and biological properties including enhanced bioactivity, increased stability, and strengthened intramolecular interactions compared with their linear analogues.[5,6] However, ring closing reactions with chirality induction face considerable difficulties due to the massive entropic penalty associated with stereoselective ring closure.[7−11] Preorganization of linear substrates through hydrogen bonding interactions or confinement using chiral container structures, such as capsules and cages, can overcome this challenge by holding the substrate in a folded chiral conformation. Constrictive chiral folding can facilitate the ring closing reaction with chirality induction. Previously, we have demonstrated that the macrocyclization of a linear substrate under confinement in a chiral capsule assembly can generate a chiral macrocycle product with high enantioselectivity.[12] In addition, when a macrocyclization is performed under confinement in switchable chiral capsules, the enantioselectivity can be precisely controlled by applying sonication.[13] Despite the remarkable progress that has been made using a confinement strategy, the induction of multiple chirality in a macrocyclization event remains elusive. The multiple chirality induction with high levels of stereoselectivity requires the combination of an enantioselective reaction step and an additional diastereoselective step, which is major hurdle in the synthesis of a macrocycle bearing multiple chirality.[14−20] Thus, an important goal would be the construction of confined chiral spaces that are able to perform ring-forming reactions to install multiple chiralities in a single transformation with high levels of stereoselectivity. To address this challenge, we envisioned that chiral fixation of a linear substrate including multiple prochiral moieties into a chiral space would dictate absolute and relative configurations of stereoisomers because a fixed conformation simultaneously holds a chiral conformer associated with chain folding and a spatial orientation of the prochiral moiety inside a chiral space. The fixed spatial orientation of the prochiral group would allow preferential exposure of one face over the opposite face for nucleophilic attack to generate a stereocenter. In addition, ring closure creates a short bridge that restricts free rotation around specific C−C bonds to stabilize a preferential atropisomeric or helical conformer, thereby generating strain-induced chirality such as axial, planar, or helical chirality.[21] Thus, the ring closing reaction of a linear substrate would induce multiple chirality, including a stereocenter and strain-induced chirality in a single-step macrocyclization process (Figure 1).

To explore multiple chirality induction under chiral confinement in a single step, the rational design of chiral space is essential for substrates to adopt fixed multiple chiral conformations. Among diverse chiral spaces for confined chemical reactions,[22−27] single-layered porous sheet structures would be best fit to perform confined chiral reactions with high efficiency because all of the pores in a single layer are uniformly open to the surrounding environment without pore blocking.[28−30] Moreover, when macrocyclizations are completed,

Received: June 13, 2025
Revised: August 7, 2025
Accepted: August 7, 2025
Published: August 13, 2025

https://doi.org/10.1021/jacs.5c09981
J. Am. Chem. Soc. 2025, 147, 31198−31203

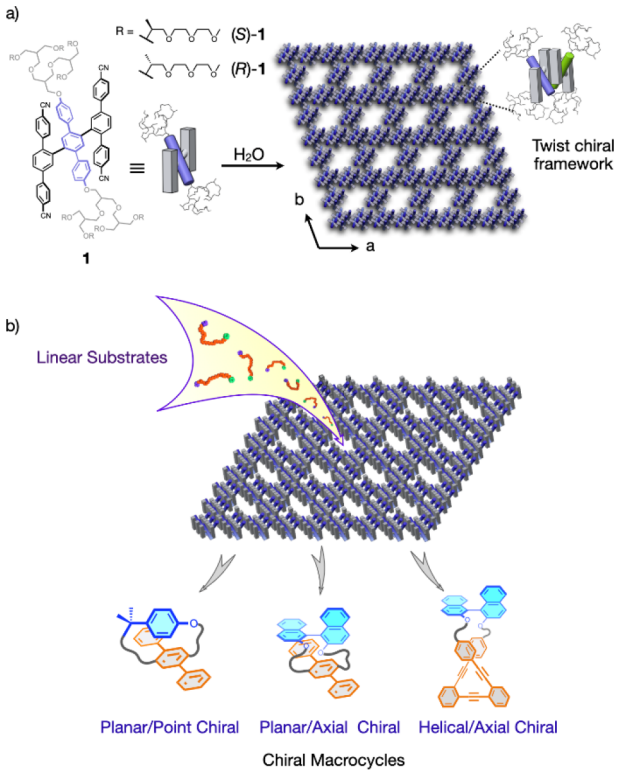

Figure 1. (a) Self-assembly of **1** into a chiral porous sheet in an aqueous solution. Two neighboring central rods in the sheet assembly twist relative to each other, giving rise to supramolecular chirality. (b) Schematic illustration of the simultaneous induction of various double chiralities in a single-step macrocyclization under chiral confinement.

the products can be spontaneously released out of the open pores without a tedious washing process due to a decrease in hydrodynamic volume caused by ring closure.

RESULTS AND DISCUSSION

Design and Characterization of Chiral Porous Nanosheets. With this in mind, we designed and prepared homochiral porous sheet structures with an in-plane hexagonal order using the self-assembly of aromatic amphiphile **1**. Molecule **1** features a planar aromatic building block in the shape of a parallelogram plate and hydrophilic chiral dendrons grafted at both ends of a central aromatic rod (Figure 1a). The terphenyl side groups in the molecule can lead **1** to form a stable self-assembly through aromatic interactions with additional dipolar interactions due to electron-withdrawing CN groups at their end parts. The central rod in the aromatic plane would be tilted by rotation out of the aromatic plane due to bulky dendrimers grafted at both ends. Owing to the bulkiness of the dendrimer chains, the two neighboring central rods in the sheet assembly are twisted against each other with respect to the side triphenylene units, thus generating supramolecular chirality.[31] The aromatic amphiphile was synthesized from commercially available starting materials in a stepwise manner. The resulting amphiphilic molecule was characterized by NMR spectroscopy and MALDI-TOF mass spectroscopy (Figures S22 and S24), which were shown to be consistent with the chemical structure presented. The aromatic amphiphile based on hydrophilic chains self-assembles into a single-layer porous 2D sheet structure in the aqueous solution. The transmission electron microscopy (TEM) images with negatively stained films revealed flat 2D sheet structures with an in-plane hexagonal order, indicating that the 2D sheet structures consist of in-plane ordered pores (Figure 2a). Selected area

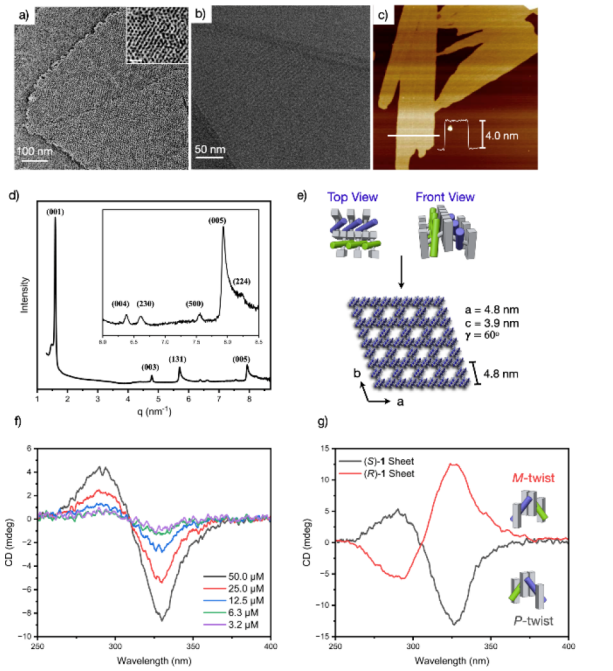

Figure 2. (a) Negatively stained TEM image of **1** (50 μM) in a water solution. Inset: high-resolution TEM image showing in-plane ordered pores (scale bar: 20 nm). (b) Cryo-TEM image of **1** (50 μM) in the water solution. (c) AFM height image of the film on a mica surface from evaporation of **1** (50 μM) in the water solution. (d) SAXS pattern of **1** with a freeze-dried sample. (e) Schematic illustration of the porous sheet structure formed by the self-assembly of **1**. (f) CD spectra of (*S*)-**1** in water at different concentrations. (g) CD spectra of (*S*)-**1** (black) and (*R*)-**1** (red) in water (50 μM).

electron diffraction (SAED, Figure S72) analysis showed hexagonal symmetry with an in-plane dimension of 4.8 nm. The formation of stable sheet structures in aqueous solutions was further confirmed by cryogenic transmission electron microscopy (cryo-TEM, Figure 2b and Figure S71). Atomic force microscopy (AFM) analysis showed that the nanosheets are very flat, with a uniform thickness of 4.0 nm (Figure 2c). The porous structure was further supported by density measurements (Table S1) of the films that showed to be 0.997 g/cm^3, much lower than the expected value from closely packed 2D aggregates without empty inner spaces.[32]

To obtain more detailed information about the 2D sheet structure, X-ray experiments were performed with freeze-dried samples of **1**. Small-angle X-ray scatterings (SAXS) showed a number of sharp reflections that agree well with the expected peak positions for a 3D hexagonal structure with lattice parameters of a = 4.82 nm and c = 3.95 nm (Figure 2d and Figure S73). Considering the layer thickness of 4.0 nm determined from AFM, this result indicates that the single-layered porous nanosheets are stacked in an eclipsed manner. Considering the lattice parameter and the measured density, the number of molecules consisting of a pore can be calculated as 18 (Table S1), giving rise to a 2D framework array of hexameric clusters in which the central-terphenyl unit grafted by flexible chains is twisted out of the aromatic molecular plane in a preferred direction (Figure 2e). To minimize steric

https://doi.org/10.1021/jacs.5c09981
J. Am. Chem. Soc. 2025, 147, 31198−31203

hindrance between the bulky dendritic chains grafted in a central terphenyl group, the twist between adjacent central triphenyl units would be opposite to one another, giving rise to twist chirality.[31] Indeed, circular dichroism (CD) spectroscopy experiments of (*S*)-**1** revealed a strong negative Cotton effect at 327 nm (Figure 2f). When highly diluted, TEM showed the formation of discrete nanostructures (Figure S75) that are also optically active, indicating that the chiral primary structure grows in two dimensions to form a single-layered sheet with increasing concentration. The sheet solution of (*R*)-**1** formed from the enantiomeric molecule exhibits the opposite CD signal with a perfect mirror-image relationship (Figure 2g), indicating that the chirality of the dendrimer chain is communicated to the packing of aromatic stacks, generating chiral 2D sheet structures. Considering the estimated curve by calculations, the chirality of the sheet formed from (*S*)-**1** can be assigned as a *P*-form, while that of the sheet from (*R*)-**1** can be assigned as an *M*-form (Figure S76).

Confined Macrocyclization for Stereocenter and Planar Chirality Induction. Considering the alternative twisting of the central triphenylene units in opposite directions, the 2D networks consisting of discrete cluster arrangements endow the internal aromatic pores with a chiral interior. Accordingly, the internal cavity of the 2D porous sheet structure would function as a collective chiral reactor in aqueous environments.[13] When the chiral pore uptakes a linear substrate, the substrate would adopt a folded chiral conformation inside the chiral cavity, a preorganized structure for a chiral macrocyclization. Moreover, the chiral wall of the internal cavity enables the prochiral end group to be fixed in its spatial orientation. Thus, the macrocyclization of a linear substrate including a prochiral end group under chiral confinement would allow access to multiple chirality inductions in a single-step macrocyclization process. To corroborate the capability of the chiral porous sheet to induce chirality in a macrocyclization process, we selected hydrophobic linear substrate **L1** including a prochiral end group for Michael reaction (Figure 3a). Fluorescence quenching titration experiments with the *P*-sheet showed that each pore is occupied by a single substrate with ~96% uptake (Figure 3b and Figure S78 and S83), indicative of well-fit of the substrate with a constrictive conformation into a chiral cavity. Consistent with fluorescence quenching, 1D NOE measurements with selective irradiation on H_1 showed a prominent peak at 6.48 ppm associated with the coupling between (*S*)-**1** and substrate **L1** (Figure 3c and Figure S81). Furthermore, NOE signals associated with intramolecular coupling between the end groups of the linear substrate can be clearly visualized at 6.6 and 6.8 ppm, respectively, indicative of a close fit of the linear substrate with preorganized folding into the chiral pore. It is worth noting that the CD signal of the sheets remains unchanged even after entrapping the substrate (Figure S77), demonstrating that the pore chirality is retained without being compromised by substrate encapsulation. These observations indicate that the entrapped linear substrate adopts a fixed chiral conformation with a preferential orientation of the prochiral C−C double bond. Thus, the confined reaction of **L1** would induce a stereocenter in a single-step macrocyclization process.[12] To confirm this, we performed the Michael reaction of entrapped **L1** in the *P*-sheet by addition of a catalytic amount of triflic acid (1 mol % relative to **L1**). When subjected to analytical HPLC, a single additional peak corresponding to a macrocycle product was identified in analytical HPLC in which

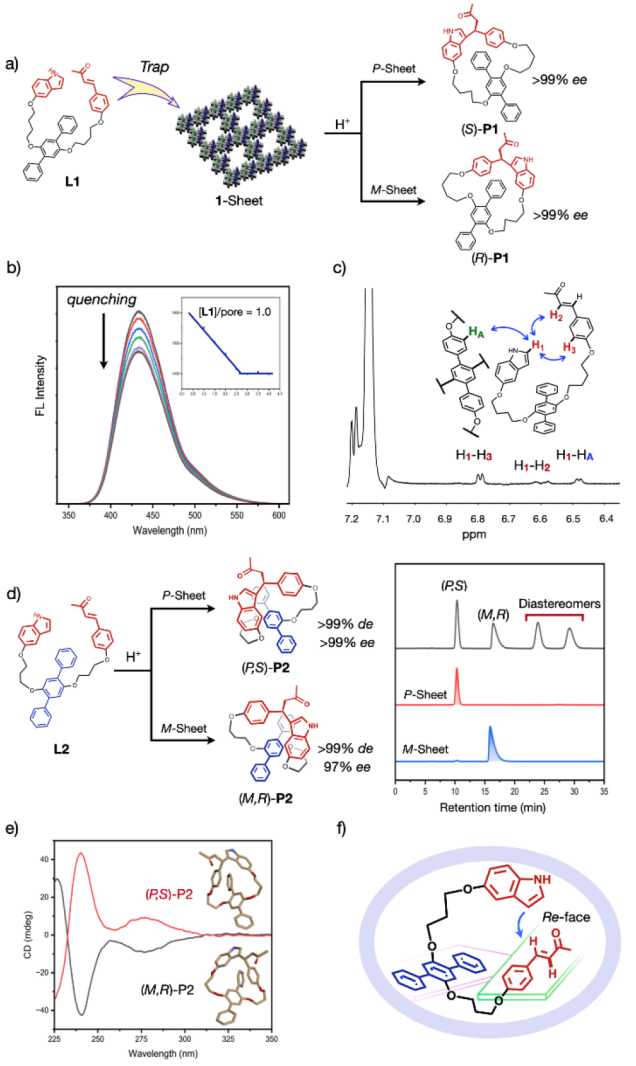

Figure 3. (a) Macrocyclization of **L1** in the presence of the *P*-sheet and *M*-sheet. (b) Fluorescence titration spectra of **L1** based on 45 μM **1** in aqueous solutions. Inset: fluorescence intensity dependence at 426 nm on concentration of **L1**. (c) Partial 1D NOE spectrum (600 MHz, 298 K) of (*S*)-**1** (900 μM) and guest **L1** (50 μM) in D_2O/THF-d_8/MeOH-d_4 (8:1:1, v/v/v) (irradiation at 7.15 ppm corresponded to proton H_1). (d) Macrocyclization of **L2** and chiral HPLC traces of **P2** obtained from a standard reaction (top), a reaction in the presence of the *P*-sheet (middle), and a reaction in the presence of the *M*-sheet (bottom), respectively. (e) CD spectra and single-crystal X-ray structures of (*P*,*S*)-**P2** (red) and (*M*,*R*)-**P2** (black). (f) Energy-minimized structure of **L2** in a confined chiral space of the *P*-sheet.

the intensity increases gradually at the expense of **L1** and then levels off at 3 h (Figures S84 and S85), indicating that the reaction proceeds to yield a clean macrocycle product.

Remarkably, the chiral HPLC profile of the macrocycle shows a single peak associated with one enantiomeric macrocycle, demonstrating that the confined reaction proceeds to selectively form only one enantiomer with an excellent enantioselectivity (*ee* > 99%) (Figure 3a and Figure S86). CD measurements of the enantiopure product showed a negative Cotton effect at a longer wavelength; thus, the absolute configuration of a stereocenter can be assigned as an (*S*)-form considering the estimated curve by calculations (Figure S87). When a control experiment is performed in the absence of the porous sheet structure, the macrocyclization generates a pair of

https://doi.org/10.1021/jacs.5c09981
J. Am. Chem. Soc. 2025, 147, 31198−31203

stereoisomers, indicating that **P1** has a stereocenter with a lack of planar chirality. A lack of planar chirality in the macrocycle compound implies that the butyl bridge in the **P1** ring is not sufficiently short to restrict the rotation of the terphenyl unit, leading to a macrocycle bearing only a stereocenter. As expected, the confined macrocyclization of **L1** using an *M*-sheet yielded an (*R*)-stereocenter, an opposite enantiomeric macrocycle without loss of enantiopurity (Figure S86).

To generate strain-induced chirality by restricted rotation of the terphenyl group, we considered the Michael reaction of **L2** based on a shorter alkyl chain (propyl group), which can result in the formation of configurationally stable isomers. Indeed, control experiments of **L2** in the absence of the 2D sheet structures showed the formation of all four possible diastereomers different from **L1** (Figure 3d), illustrating that the linear substrate with a shorter alkyl chain can induce planar chirality in addition to a stereocenter during a ring closing reaction.[33] To confirm the selective formation of one diastereomer among four possible stereoisomers, we performed a macrocyclization after encapsulation of **L2** in the chiral cavity of the *P*-sheet (uptake: 98%, Figure S88). Notably, the confined reaction generates a clean macrocycle product of a pure diastereomer (*P*,*S*-form), demonstrating that the chiral porous sheet allows access to the installation of multiple chirality in a macrocycle skeleton with excellent diastereo- and enantioselectivities (*de* > 99% and *ee* > 99%) (Figures S89–S91). The absolute configuration of the chiral macrocycle was established unequivocally by using single-crystal X-ray crystallography (Figure 3e, inset). Due to the inflexibility of the ring structure, the macrocyclization of the substrate would be accompanied by the induction of planar chirality in the cyclic skeleton. In addition, the restricted rotation of the prochiral end group inside the chiral cavity endows it with the preferential exposure of one face over the other toward an indole nucleophile, generating a stereocenter during the ring closing event. Consequently, the confined reaction of **L2** proceeds with the simultaneous induction of both planar chirality and a stereocenter in a single-step transformation. Indeed, the energy-minimized structure of **L2** in the *P*-sheet shows that the addition of indole to the *Re*-face of an unsaturated carbonyl group is favored to yield **P2** macrocycle with (*P*)-planar chirality and (*S*)-stereocenter, which explains the observed stereoselectivity (Figure 3f and Figure S103). When the *M*-sheet is used, the confined reaction of **L2** produces an opposite enantiomeric macrocycle (*M*,*R*-form) (Figure 3d and Figure S91). This result demonstrates that enantioselectivity in macrocyclization with multiple chirality induction can be precisely controlled by using the chiral porous sheet assembly.

Generation of Macrocycles with Axial and Helical Chirality. When the end groups of linear substrate **L2** are replaced by 1-naphthyl groups (**L3**), the macrocyclization can generate C–C axial chirality due to restricted rotation around a single bond in the 1,1'-binaphthyl group in the cyclic skeleton (Figure 4a). Although binaphthyl derivatives as chiral building blocks are widely employed for constructing chiral macrocycles with distinctive optical properties,[34] the atroposelective formation of binaphthyl groups during macrocyclization remains a challenge.[35] Indeed, the confined macrocyclization of naphthyl-functionalized linear substrate **L3** in the *P*-sheet yields (*P*,*R*)-**P3** with an excellent stereoselectivity, while the *M*-sheet produces an opposite enantiomeric macrocycle, (*M*,*S*)-**P3**, demonstrating that a confined coupling reaction can induce simultaneously axial and planar chirality (Figure 4b and Figures S94–S97).

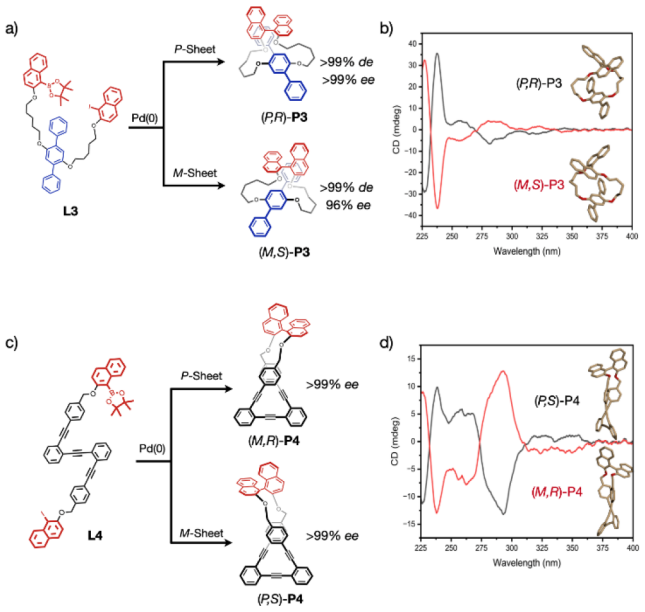

Figure 4. (a) Chiral macrocyclization of **L3** by intramolecular Suzuki coupling reaction in the presence of the *P*-sheet (top) and *M*-sheet (bottom). (b) CD spectra and single-crystal X-ray structures of (*P*,*R*)-**P3** (black) and (*M*,*S*)-**P3** (red). (c) Chiral macrocyclization of **L4** in the presence of the *P*-sheet (top) and *M*-sheet (bottom). (d) CD spectra and single-crystal X-ray structures of (*M*,*R*)-**P4** (red) and (*P*,*S*)-**P4** (black).

To apply this approach to induce additional strain-induced chirality in a ring closing reaction, we selected substrate **L4** in which cyclization would induce double chirality based on a helical structure (Figure 4c). The enantioselective macrocyclization of **L4** would fix a preferred helical conformation of a linear chain under chiral confinement to generate a configurationally stable structure; thus, a single-step transformation would simultaneously install double chirality including helical chirality in addition to axial chirality. Control macrocyclization experiments generate only two enantiomers with a lack of diastereomers, different from the case of **L3**. This is most probably because the *R*/*S* axial chirality is dictated by the helical chirality of the ortho-oligo(phenylene) ethynylene (OPE) group due to a biased equilibrium between *R*- and *S*-forms.[36,37] Thus, *P*-helicity couples with *S*-axial chirality, while *M*-helicity generates *R*-axial chirality. Indeed, the aromatic coupling reaction of **L4** in the *P*-sheet by addition of the catalyst yields a highly enantiopure macrocycle product with (*R*)-axial chirality and *M*-helicity without any traces associated with an opposite enantiomer (Figures S99–S101), indicating that the confinement approach is an excellent method to induce helical chirality in addition to axial chirality with an exquisite selectivity in a single-step macrocyclization process. CD of the macrocycle formed in the *P*-sheet shows a negative Cotton effect at the longest wavelength, characteristic of *M*-helicity, which is a good agreement with the calculated CD spectrum (Figure 4d and Figure S102).[38] The absolute configuration was also unambiguously confirmed by single-crystal X-ray crystallography (Figure 4d, inset), demonstrating that the macrocyclization in the *P*-sheet generates simultaneously *M*-helical and *R*-axial chirality. Meanwhile, the identical reaction in the *M*-sheet yields a (*P*,*S*)-macrocycle,

https://doi.org/10.1021/jacs.5c09981
J. Am. Chem. Soc. 2025, 147, 31198–31203

indicating that the pore chirality dictates absolute configuration in a macrocyclization. Covalent stitching of folded helical structure into a macrocyclic framework provides a means to achieve the configurational stability, which is an important step toward interrogation of chiroptical properties of aromatic helices. New properties can emerge in a macrocyclic environment as a result of its impact on molecular topology and spatial orientation of conjugated aromatic units.[39] In this respect, our strategy to stabilize a helical conformation via covalent fixation under chiral confinement can be highly useful for the facile synthesis of macrocycles bearing helical chirality in addition to axial chirality with unique chiroptical activity.

CONCLUSIONS

In summary, encapsulation of a linear substrate into a single layer of chiral porous materials and then confined macrocyclization, as demonstrated here, provides easy access to the synthesis of macrocycles bearing multiple chirality with extremely high stereoselectivity in a single-pot operation. The chiral interior of a 2D porous structure imprints its stereochemistry on the conformation of a linear substrate, enabling the substrate to simultaneously hold a chiral conformer associated with chain folding and a spatial orientation of the prochiral moiety. Thus, the ring closing reaction induces simultaneous multiple chirality, including a stereocenter and strain-induced chirality. We anticipate that such a pure confinement strategy will provide new insight into the facile stereoselective synthesis of complex macrocycles bearing multiple chirality, applicable to a wide range of chiroptical and biological applications.

ASSOCIATED CONTENT

Supporting Information

The Supporting Information is available free of charge at https://pubs.acs.org/doi/10.1021/jacs.5c09981.

General experimental procedures, synthesis of molecules, NMR data, HRMS data, TEM images, AFM images, and all other spectroscopy data (PDF)

Accession Codes

Deposition Numbers 2457568 and 2457572−2457573 contain the supplementary crystallographic data for this paper. These data can be obtained free of charge via the joint Cambridge Crystallographic Data Centre (CCDC) and Fachinformationszentrum Karlsruhe Access Structures service.

AUTHOR INFORMATION

Corresponding Authors

Zhanting Li − *Shanghai Institute of Organic Chemistry (SIOC), Shanghai 200032, China;* orcid.org/0000-0003-3954-0015; Email: ztli@fudan.edu.cn

Myongsoo Lee − *Department of Chemistry, State Key Lab of Molecular Engineering of Polymers, and Shanghai Key Lab of Molecular Catalysis and Innovative Materials, Fudan University, Shanghai 200438, China;* orcid.org/0000-0002-5315-3807; Email: mslee@fudan.edu.cn

Authors

Yongsheng Li − *Department of Chemistry, State Key Lab of Molecular Engineering of Polymers, and Shanghai Key Lab of Molecular Catalysis and Innovative Materials, Fudan University, Shanghai 200438, China;* orcid.org/0009-0002-7459-0771

Tianyi Zheng − *Department of Chemistry, State Key Lab of Molecular Engineering of Polymers, and Shanghai Key Lab of Molecular Catalysis and Innovative Materials, Fudan University, Shanghai 200438, China;* orcid.org/0009-0009-6250-5075

Young Yong Kim − *Pohang Accelerator Laboratory, POSTECH, Pohang 37673, Korea*

Complete contact information is available at: https://pubs.acs.org/10.1021/jacs.5c09981

Notes

The authors declare no competing financial interest.

ACKNOWLEDGMENTS

This work was supported by National Natural Science Foundation of China (grant nos. 92156023, 92356306, and 22150710515).

REFERENCES

(1) Atanasov, A. G.; Zotchev, S. B.; Dirsch, V. M.; International Natural Product Sciences Taskforce; Supuran, C. T. Natural products in drug discovery: advances and opportunities. *Nat. Rev. Drug Discovery* **2021**, *20*, 200−216.

(2) Driggers, E. M.; Hale, S. P.; Lee, J.; Terrett, N. K. The exploration of macrocycles for drug discovery - an underexploited structural class. *Nat. Rev. Drug Discovery* **2008**, *7*, 608−624.

(3) Campos, K. R.; Coleman, P. J.; Alvarez, J. C.; Dreher, S. D.; Garbaccio, R. M.; Terrett, N. K.; Tillyer, R. D.; Truppo, M. D.; Parmee, E. R. The importance of synthetic chemistry in the pharmaceutical industry. *Science* **2019**, *363*, No. eaat0805.

(4) Garcia Jimenez, D.; Poongavanam, V.; Kihlberg, J. Macrocycles in drug discovery - learning from the past for the future. *J. Med. Chem.* **2023**, *66* (8), 5377−5396.

(5) Villar, E. A.; Beglov, D.; Chennamadhavuni, S.; Porco, J. A.; Kozakov, D.; Vajda, S.; Whitty, A. How proteins bind macrocycles. *Nat. Chem. Biol.* **2014**, *10* (9), 723−731.

(6) Mallinson, J.; Collins, I. Macrocycles in new drug discovery. *Future Med. Chem.* **2012**, *4* (11), 1409−1438.

(7) Martí-Centelles, V.; Pandey, M. D.; Burguete, M. I.; Luis, S. V. Macrocyclization reactions: the importance of conformational, configurational, and template-induced preorganization. *Chem. Rev.* **2015**, *115* (16), 8736−8834.

(8) Zheng, K.; Hong, R. Stereoconfining macrocyclizations in the total synthesis of natural products. *Nat. Prod. Rep.* **2019**, *36* (11), 1546−1575.

(9) López, R.; Palomo, C. Planar chirality: a mine for catalysis and structure discovery. *Angew. Chem., Int. Ed.* **2022**, *61* (13), No. e202113504.

(10) Mortensen, K. T.; Osberger, T. J.; King, T. A.; Sore, H. F.; Spring, D. R. Strategies for the diversity-oriented synthesis of macrocycles. *Chem. Rev.* **2019**, *119* (17), 10288−10317.

(11) Xu, S.; Arimoto, H. Strategies for construction of the all-carbon macrocyclic skeleton of the ansamycin antibiotic-kendomycin. *J. Antibiot.* **2016**, *69* (4), 203−212.

(12) Sun, B.; Shen, B.; Urushima, A.; Liu, X.; Feng, X.; Yashima, E.; Lee, M. Asymmetric transformation driven by confinement and self-release in single-layered porous nanosheets. *Angew. Chem., Int. Ed.* **2020**, *59* (50), 22690−22696.

(13) Tan, L.; Sun, M.; Wang, H.; Wang, J.; Kim, J.; Lee, M. Enantiocontrolled macrocyclization by encapsulation of substrates in chiral capsules. *Nat. Synth.* **2023**, *2*, 1222−1231.

(14) Krautwald, S.; Sarlah, D.; Schafroth, M. A.; Carreira, E. M. Enantio- and diastereodivergent dual catalysis: α-allylation of branched aldehydes. *Science* **2013**, *340* (6136), 1065−1068.

(15) Krautwald, S.; Carreira, E. M. Stereodivergence in asymmetric catalysis. *J. Am. Chem. Soc.* **2017**, *139* (16), 5627−5639.

(16) Bhaskararao, B.; Sunoj, R. B. Origin of stereodivergence in cooperative asymmetric catalysis with simultaneous involvement of two chiral catalysts. *J. Am. Chem. Soc.* **2015**, *137* (50), 15712−15722.
(17) Beletskaya, I. P.; Nájera, C.; Yus, M. Stereodivergent catalysis. *Chem. Rev.* **2018**, *118* (10), 5080−5200.
(18) Zhou, Q.; Chin, M.; Fu, Y.; Liu, P.; Yang, Y. Stereodivergent atom-transfer radical cyclization by engineered cytochromes P450. *Science* **2021**, *374* (6575), 1612−1616.
(19) Kim, B.; Kim, Y.; Lee, S. Y. Stereodivergent carbon-carbon bond formation between iminium and enolate intermediates by synergistic organocatalysis. *J. Am. Chem. Soc.* **2021**, *143* (1), 73−79.
(20) Kassem, S.; Lee, A. T. L.; Leigh, D. A.; Marcos, V.; Palmer, L. I.; Pisano, S. Stereodivergent synthesis with a programmable molecular machine. *Nature* **2017**, *549*, 374−378.
(21) Gulder, T.; Baran, P. S. Strained cyclophane natural products: macrocyclization at its limits. *Nat. Prod. Rep.* **2012**, *29* (8), 899−934.
(22) Lu, Z. F.; Ronson, T. K.; Heard, A. W.; Feldmann, S.; Vanthuyne, N.; Martinez, A.; Nitschke, J. R. Enantioselective fullerene functionalization through stereochemical information transfer from a self-assembled cage. *Nat. Chem.* **2023**, *15* (3), 405−412.
(23) Nishioka, Y.; Yamaguchi, T.; Kawano, M.; Fujita, M. Asymmetric [2 + 2] olefin cross photoaddition in a self-assembled host with remote chiral auxiliaries. *J. Am. Chem. Soc.* **2008**, *130*, 8160−8161.
(24) Li, X.; Wu, J.; He, C.; Meng, Q.; Duan, C. Asymmetric Catalysis within the Chiral Confined Space of Metal−Organic Architectures. *Small* **2019**, *15*, No. 1804770.
(25) Wang, K.; Jordan, J. H.; Hu, X.-Y.; Wang, L. Supramolecular Strategies for Controlling Reactivity within Confined Nanospaces. *Angew. Chem., Int. Ed.* **2020**, *59*, 13712−13721.
(26) Bierschenk, S. M.; Pan, J. Y.; Settineri, N. S.; Warzok, U.; Bergman, R. G.; Raymond, K. N.; Toste, F. D. Impact of Host Flexibility on Selectivity in a Supramolecular Host-Catalyzed Enantioselective aza-Darzens Reaction. *J. Am. Chem. Soc.* **2022**, *144*, 11425−11433.
(27) Dong, J.; Liu, Y.; Cui, Y. Supramolecular Chirality in Metal-Organic Complexes. *Acc. Chem. Res.* **2021**, *54*, 194−206.
(28) Liu, X.; Zhou, X.; Shen, B.; Kim, Y.; Wang, H.; Pan, W.; Kim, J.; Lee, M. Porous Nanosheet Assembly for Macrocyclization and Self-Release. *J. Am. Chem. Soc.* **2020**, *142*, 1904−1910.
(29) Feng, X.; Shen, B.; Sun, B.; Kim, J.; Liu, X.; Lee, M. Single-Layered Chiral Nanosheets with Dual Chiral Void Spaces for Highly Efficient Enantiomer Absorption. *Angew. Chem., Int. Ed.* **2020**, *59*, 11355−11359.
(30) Sun, B.; Kim, Y.; Wang, Y.; Wang, H.; Kim, J.; Liu, X.; Lee, M. Homochiral porous nanosheets for enantiomer sieving. *Nat. Mater.* **2018**, *17*, 599−604.
(31) Miyata, M.; Tohnai, N.; Hisaki, I.; sasaki, T. Generation of Supramolecular Chirality around Twofold Rotational or Helical Axes in Crystalline Assemblies of Achiral Components. *Symmetry* **2015**, *7*, 1914−1928.
(32) Lee, M.; Cho, B.-K.; Jang, Y.-G.; Zin, W.-C. Spontaneous Organization of Supramolecular Rod-Bundles into a Body-Centered Tetragonal Assembly in Coil-Rod-Coil Molecules. *J. Am. Chem. Soc.* **2000**, *122*, 7449.
(33) Tan, L.; Zheng, T.; Li, Y.; Lee, M. Stereodivergent Macrocyclization in Dynamic Chiral Confinement. *Chem.—Eur. J.* **2025**, *31*, No. e202404207.
(34) Yu, Y.; Hu, Y.; Ning, C.; Shi, W.; Yang, A.; Zhao, Y.; Cao, Z. Y.; Xu, Y.; Du, P. BINOL-Based Chiral Macrocycles and Cages. *Angew. Chem., Int. Ed.* **2024**, *63*, No. e202407034.
(35) da Silva, E. M.; Vidal, H. D. A.; Januário, M. A. P.; Corrêa, A. G. Advances in the Asymmetric Synthesis of BINOL Derivatives. *Molecules* **2023**, *28* (1), 12.
(36) Reiné, P.; Justicia, J.; Morcillo, S. P.; Abbate, S.; Vaz, B.; Ribagorda, M.; Orte, Á.; Álvarez de Cienfuegos, L.; Longhi, G.; Campaña, A. G.; et al. Pyrene-Containing ortho-Oligo(phenylene)-ethynylene Foldamer as a Ratiometric Probe Based on Circularly Polarized Luminescence. *J. Org. Chem.* **2018**, *83*, 4455−4463.
(37) Fuentes, N.; Martin-Lasanta, A.; de Cienfuegos, L. A.; Robles, R.; Choquesillo-Lazarte, D.; Garcia-Ruiz, J. M.; Martinez-Fernandez, L.; Corral, I.; Ribagorda, M.; Mota, A. J.; Cardenas, D. J.; Carreno, M. C.; Cuerva, J. M. Versatile Bottom-up Approach to Stapled p-Conjugated Helical Scaffolds: Synthesis and Chiroptical Properties of Cyclic o-Phenylene Ethynylene Oligomers. *Angew. Chem., Int. Ed.* **2012**, *51*, 13036−13040.
(38) Ortuño, A. M.; Reiné, P.; Resa, S.; Álvarez de Cienfuegos, L.; Blanco, V.; Paredes, J. M.; Mota, A. J.; Mazzeo, G.; Abbate, S.; Ugalde, J. M.; et al. Extended enantiopure ortho-phenylene ethylene (o-OPE)-based helical systems as scaffolds for supramolecular architectures: a study of chiroptical response and its connection to the CISS effect. *Org. Chem. Front.* **2021**, *8* (18), 5071−5086.
(39) Xue, Y.; Shi, Y.; Chen, P. Circularly Polarized Luminescent p-Conjugated Chiral Nanorings and Nanobelts. *Adv. Opt. Mater.* **2024**, *12*, No. 2303322.

https://doi.org/10.1021/jacs.5c09981
J. Am. Chem. Soc. 2025, 147, 31198−31203